SLAC – PUB – 3816
October, 1985
(N)

THE RECENT OPERATIONAL PERFORMANCE OF THE CERN OMEGA RING IMAGING ČERENKOV DETECTOR*

R. J. APSIMON, P. S. FLOWER,
K. A. FREESTON, G. D. HALLEWELL, *
J. A. G. MORRIS, J. V. MORRIS, C. N. PATERSON,
P. H. SHARP, AND C. N. UDEN

Rutherford Appleton Laboratory, Chilton, Didcot, Ozon 0X11 0QX United Kingdom

M. DAVENPORT AND J. EADES

CERN, CH-1211, Geneva 23, Switzerland

P. A. COYLE AND D. MERCER

University of Manchester, Schuster Laboratory, Manchester M13 9PL, United Kingdom

and

S. DANAHER†, R. H. MCCLATCHEY,‡
N. THACKER AND L. F. THOMPSON

University of Sheffield, The Hicks Building, Sheffield S3 7RH, United Kingdom

ABSTRACT

We discuss the design and construction of the Time Projection chambers (TPCs) of the Omega Ring Imaging Čerenkov Detector (RICH). Details are given of the TPC high voltage system and its monitoring and control. In addition, the operation and monitoring of the readout is described together with results of tests on the performance of the front end amplifiers.

The operation of the RICH TPCs and electronics during the first data run of WA69, in 1984, is discussed together with relevant results from laboratory tests. Results from the preliminary analysis of a sample of data from the 1984 run are also presented.

1. INTRODUCTION

Figure 1 shows a general view of the RICH in the WA69 high energy photo production experiment at the CERN Omega Spectrometer.

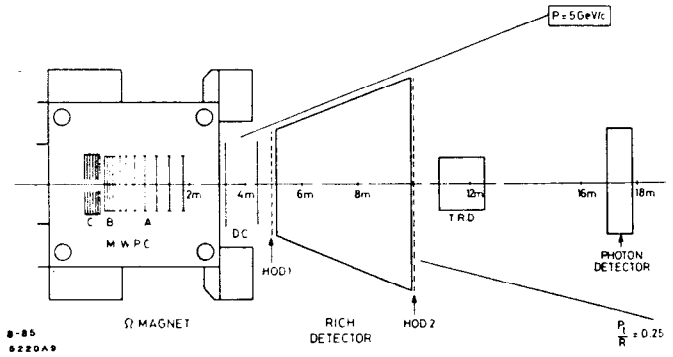

Fig. 1. View of the RICH in WA69.

Secondary particles from interactions in the spectrometer enter the detector and traverse a 5 meter atmospheric pressure gas radiator (Fig. 2), producing ultraviolet Čerenkov radiation which is focussed by a 7m × 4m mirror array onto a focal surface containing 16 time projection chambers (TPCs).

In the first phase of WA69 (Summer 1984) a nitrogen radiator was used, giving pion, kaon and proton thresholds of 5, 19 and 37 GeV/c respectively, and a ring radius of 12.5 cm for $\beta = 1$ particles.[1]

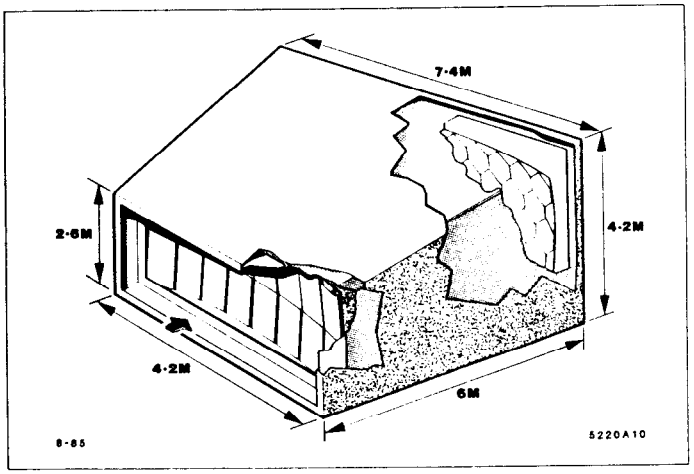

Fig. 2. General View of the RICH.

A single TPC is shown in plan and elevation in Fig. 3. Čerenkov photons enter the TPC through an ultraviolet transmitting window of Suprasil II fused silica[♯1] ("quartz"). The gas mixture in the TPCs was 80% methane (CH_4) and 20% isobutane (C_4H_{10}). This mixture was passed through a gas purification system to reduce the contamination from oxygen and water vapour to the level of a few parts per million, and then bubbled through the organic photoionizing liquid tetrakis (dimethylamino) ethylene (TMAE) at a temperature of 15°C. The Čerenkov photons photoionize the TMAE molecules (average ultraviolet absorption length 43 mm[2] and the resulting photoelectrons drift under the influence of an applied electric field to the central proportional wire plane (PWP).

Each of the 192 sense wires in the PWP is connected to a local preamplifier and in turn to a second stage amplifier, discriminator and time slice encoder (TSE) as shown in Fig. 4. After an event trigger, data from the TPCs are strobed into memory where they are encoded into wire number and time slice and read into CAMAC.

The number of photoelectrons seen in the detector from a Čerenkov cone angle θ developed in a radiator length L (cms)

*Work supported by the Department of Energy, contract DE-AC03-76SF00515

* Present address: Stanford Linear Accelerator Center, P. O. Box 4349, Stanford, California, 94305, U.S.A.
†School of Electrical Engineering, Leeds Polytechnic, Leeds, United Kingdom
‡CERN, CH-1211, Geneva 23, Switzerland

♯1 Manufactured by Hereaus & Co., West Germany

Presented at the Nuclear Science Symposium, San Francisco, California, October 23-25, 1985

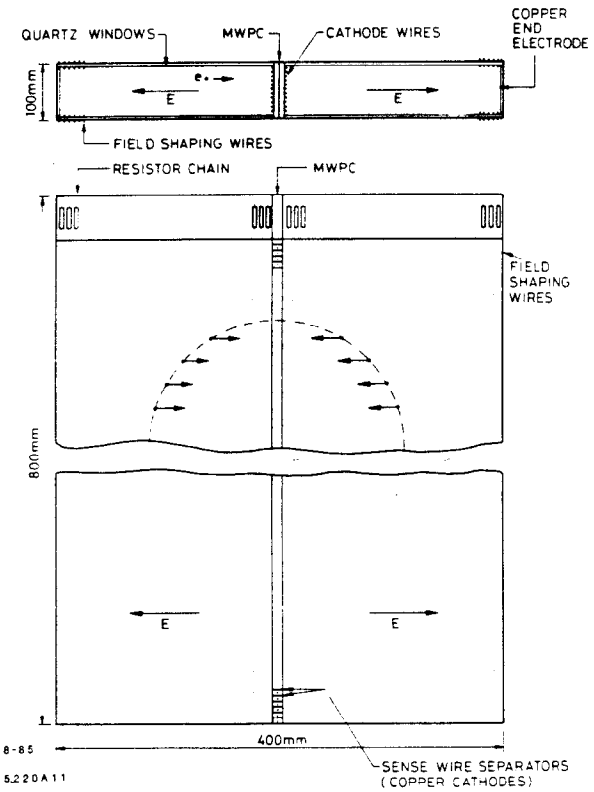

Fig. 3. Plan and Elevation of a TPC.

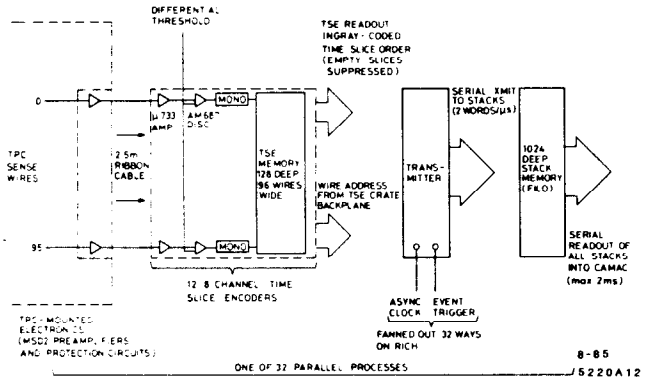

Fig. 4. Schematic of thge RICH Readout System.

is given by

$$N_e = 370 L \sin^2\theta \int Q(E)R(E)T_w(E)T_g(E)dE = N_o L \sin^2\theta$$

where E is the Čerenkov photon energy. N_o represents overall detection efficiency for Čerenkov photons and is the product of the mirror UV reflectivity R(E), the quartz window UV transmission $T_w(E)$, and TMAE quantum efficiency Q(E) and the radiator gas transmission $T_g(E)$. The value of N_o seen under actual experimental running conditions is given in §6.

2. THE TPC AND THEIR HIGH VOLTAGE SYSTEM

Each TPC consists of a 20 cm drift volume on either side of the PWP. The drift field is defined by 4 resistive chains connected in parallel at their top and bottom ends. Two chains are fitted to the quartz window, which is permanently attached to the RICH, forming part of the radiator gas enclosure. The other pair are attached to the demountable TPC, and can be easily unplugged from a high voltage distribution panel when the TPC is removed for servicing. Each chain consists of 98 1 MΩ, 1% tolerance resistors, and supplies voltage to 100μ diameter field wires mounted at 2 mm pitch on both sides of the glass and quartz windows. A negative potential-typically -11 kV[12] — is applied to the outermost field wires and also to the copper boards which form the ends of the drift volumes. The graded potentials from the wires are also connected to plated strips on double sided circuit boards, so that each potential forms two concentric closed loops around the drift volumes.

The PWP structure consists of 192 10 cm long, 20μ diameter gold plated tungsten sense wires at 4 mm pitch, separated by 0.8 mm thick copper-coated fiberglass cathodes. The separators define the anode-cathode spacing of 1.6 mm, and extend 4 mm into each drift volume to limit the solid angle for the emission of UV photons produced in the avalanches around the sense wires. To complete the PWP, 50 cathode wires of 100μ diameter were pitched at 2 mm across the entrances to all cells perpendicular to the cathode dividers. The sense wires are effectively at ground potential, being connected to the preamplifier inputs, while the cathodes are operated in the voltage range -1.8 to -2.15 kV. To protect the sense wires and their amplifiers, each cathode voltage supply cable included a current limiting series resistor. In addition, the cathode supplies[13] incorporated an over-current trip and a ramping facility which reduced their output by about 500 volts between beam gates, to quench any long term discharges within the TPCs.

In each TPC, the final drift wires were biased to a more negative potential than the PWP cathode with a variable resistance whose value was selected, in conjunction with the drift chain supply voltage, to set up the required drift field at a particular PWP operating voltage.

Figure 5 shows the circuit for a single resistance channel. Resistances are selected with "make before break" rotary switches and a potentiometer. It is necessary to prevent the voltage on the final drift wires of the TPC rising to a level — perhaps due to an incorrect resistance selection, or to an open circuit fault arising between the rotary switch contacts — where potentially damaging breakdown to the PWP would occur. The voltage is monitored via a 1000:1 divider chain by a voltage sensing relay (VSR) and compared to a reference voltage representing 1/1000 of the safe maximum. Should this be exceeded, the VSR closes a high voltage reed relay, grounding the bottom ends of the drift chains. The JFET acts as an impedance buffer between the monitor network and the low input impedance VSR.

The TPC high voltages and currents were continuously monitored by a CAMAC data logger and written to tape with the other RICH data. An on-line monitoring program warned when any voltage or current had drifted outside its permitted limits.

[12] 0 → −30 kV 1 mA Supply, Alpha Mark II Series, Brandenburg Ltd, Thornton Heath, Surrey, England

[13] P.A.G. Model 344 Regulated High Voltage power supply, Rutherford Appleton Laboratory, 1975

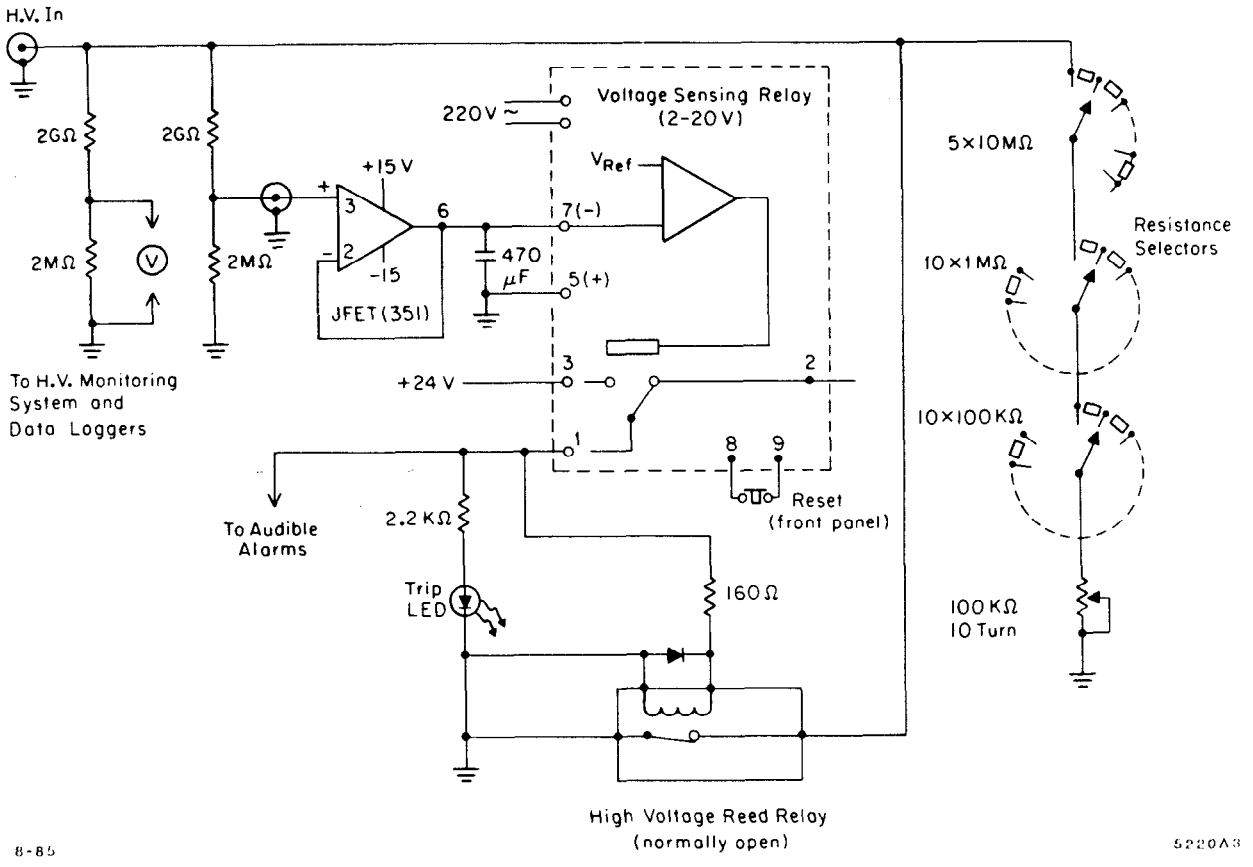

Fig. 5. A Single H. V. Resistance Channel.

3. THE RICH READOUT SYSTEM

3.a General Description

Figure 4 shows the RICH readout system in schematic form. Signals at the sense wires are received by locally-mounted preamplifiers (CERN/Laben type MSD2)[4] — guarded against discharges of up to 5 kV from 300 pf by transistor protection circuits (Fig. 6),[5] before passing to 8 channel time slice encoder modules (TSEs) containing main amplifiers (gain × 100), discriminators and 128 slice time-addressed memories.[14]

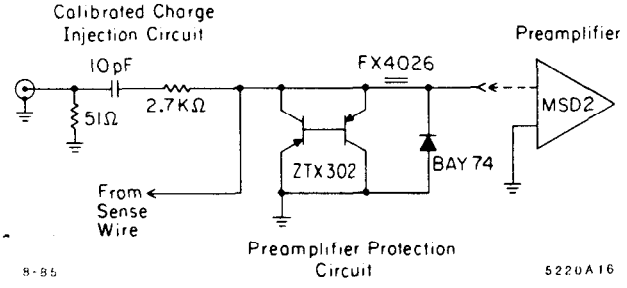

Fig. 6. Preamplifier Protection Circuit.

The TSEs operate in a circular-buffer mode, making the system sensitive to Čerenkov signals arriving before the formation of the event trigger (Fig. 7). Memory time slice widths are determined by the frequency of a high stability CAMAC-programmable clock generator. The clock frequency is chosen on the basis of the measured drift velocity and the required spatial resolution in the direction of drift. Under typical run conditions, with a drift field of 420 V/cm, the drift velocity of 3.6 cm/μs (for a gas mixture containing 80% methane, 20% isobutane and TMAE) gave a maximum drift time of $\sim$ 6 μs over 20 cm. A clock frequency of 21 MHz was generally applied, giving a drift coordinate resolution of about 1.8 mm.

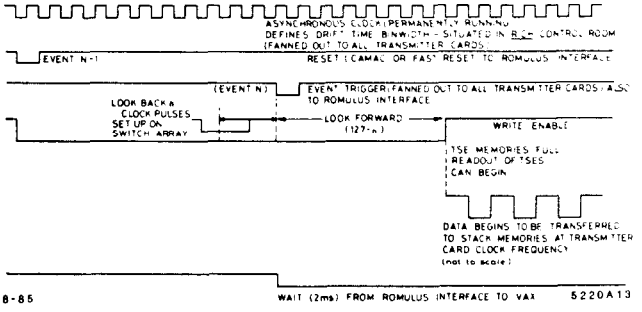

Fig. 7. RICH Readout System Timing Diagram.

The clock pulses activate a 128 step cyclic Gray code generator which sets up the memory addresses to be loaded. The

[4] Fujitsu MBM 10422 4 bit 100MHz ECL RAM

Gray-encoding of memory addresses ensures that only one bit transition occurs during each address change — minimizing the digital "noise" injected into the TSEs. Following an event trigger, the TSEs memories remain sensitive for a number of clock pulses chosen by

$$n_{ck} = 128 - (\Delta t \cdot f)$$

where f is the clock frequency and Δt is the expected time interval between the arrival of the Čerenkov light in the TPCs and the formation of the event trigger.

Data is read from the TSE memories in Gray-encoded time slice order, compressed and passed along 32 parallel streams (one for each group of 96 wires) at 2 MHz to 1024 word stack memories before being read sequentially into CAMAC.

3.*b* Amplifier Performance

The two main requirements for the TPC amplifier system were

i) adequate sensitivity to detect single photoelectrons with a TPC gas gain in the range 10^5 (§4.c).

ii) crosstalk rejection for the large signals resulting from the passage of secondary particles through the 10 cm of drift gas.

These parameters were investigated[3] by injecting calibrated amounts of charge into the system with circuits designed to simulate the shapes of pulses seen from either single photoelectrons or track ionization (Fig. 8). The amplifier charge sensitivity was measured at several TSE discriminator threshold voltages, and the charge amplification (in mV/fC) computed. In laboratory tests, noise limited the minimum practicable charge threshold to $4 \rightarrow 5fC$ (about 27000 electrons), at a corresponding discrimination level of −100 mV. An amplification of 23 mV/fC was found to give linear response for signals up to $\sim 10^6$ electrons. Although higher gain was possible, this resulted in a shorter range of linear amplification and increased interchannel crosstalk. At a TSE discriminator threshold of −375 mV (§5.b), crosstalk only became visible — as synchronous hits on the two channels adjacent to the struck wire — for signals in excess of 1.2×10^6 electrons. A sense wire that had collected the charge from an avalanche induced by several hundred ion pairs was insensitive due to amplifier saturation for a period of at least 2.5 μs to a following single photoelectron signal.

3.*c* On Line Calibration and Monitoring

The threshold voltages applied to the TSE discriminators of each half — TPC could be independently controlled, and were monitored — together with the voltages — by a CAMAC data logging system.

Pulses of known charge were injected into fiducial amplifiers in each TPC to provide an on-line calibration of the charge sensitivity at a particular TSE threshold. A common pulse was split and sent to locally-mounted pulse shapers through independently-controlled attenuators. A second test system was used to identify 'dead' readout channels by pulsing all the odd- or even-numbered channels simultaneously.

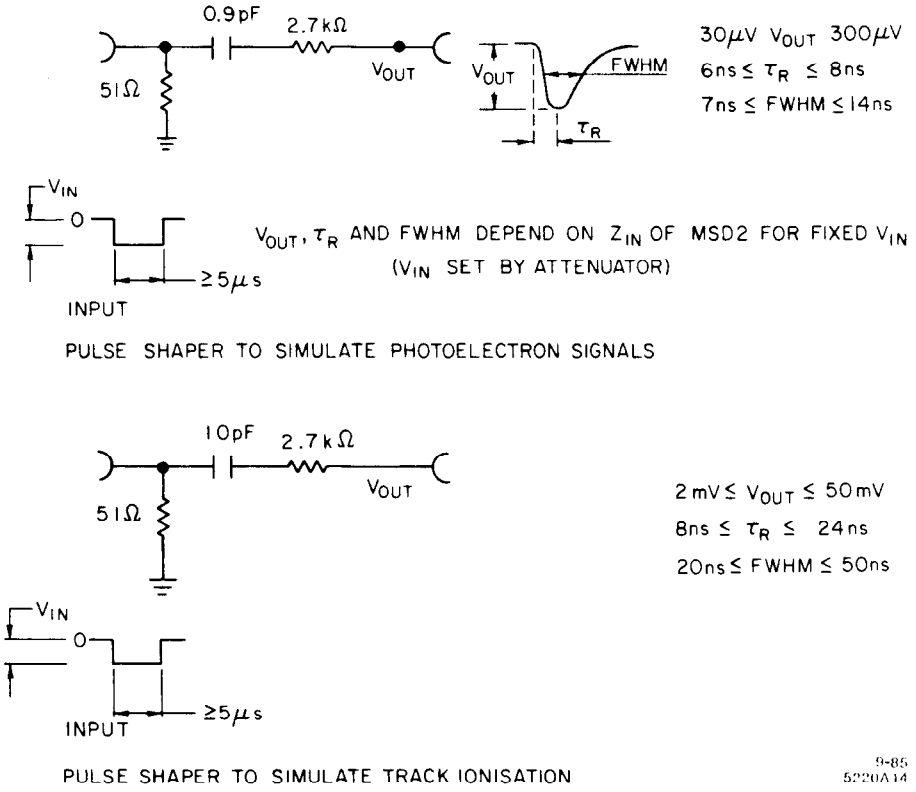

Fig. 8. Amplifier Calibration Pulse Shapers.

4. LABORATORY TESTS OF TPC PERFORMANCE

4.a Laboratory Set-up

A TPC and quartz window were mounted vertically to intercept a collimated beam of UV light from a low pressure deuterium lamp (Fig. 9). The TPC and UV beam were surveyed to ensure that the beam entered the chamber at normal incidence — parallel to the TPC sense wires.

Photoelectrons produced in the gas then drifted horizontally into the PWP cells. An inclined calcium fluoride plate reflected ~ 7% of the incident beam onto a wavelength shifted photomultiplier tube (PMT) to allow the beam intensity to be monitored. The optical elements were mounted on a traversing stage which allowed the beam to be scanned vertically and horizontally in 0.1 mm increments.

The beam, having traversed a 40 cm, air path, entered the TPC through the quartz window. Photons below 220 nm, photoionized the TMAE vapour (saturated at 10°C) and the resulting photoelectrons drifted to the PWP. The vertical profile of the photoelectron distribution was 0.9 mm FWHM after 2 cm of drift.

A group of adjacent sense wires were instrumented with standard front end preamplifiers and connected to a TSE module as shown in Fig. 9. The PMT signal was discriminated and scaled to provide a normalization rate. The singles rates on individual wires were also scaled, as was the 'OR' of the group

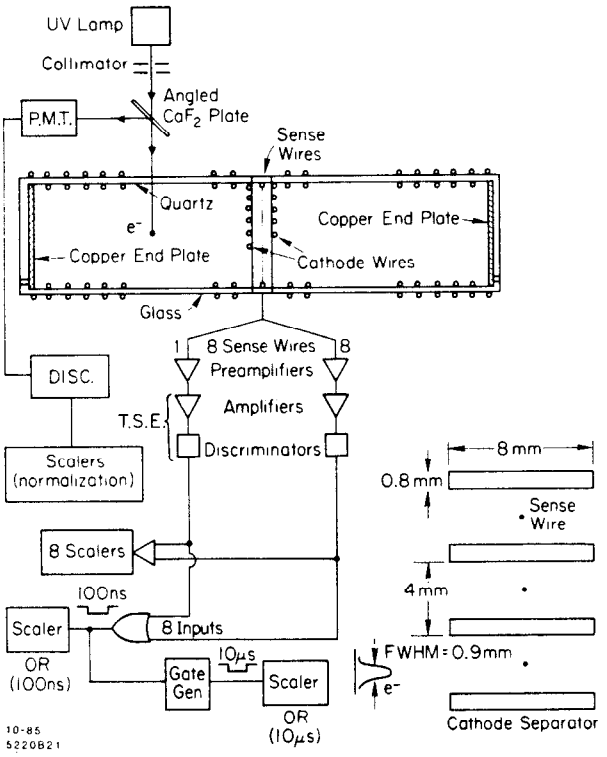

Fig. 9. TPC Laboratory Test Set-up.

of wires, using two gate widths, −100 ns and 10 μs, to alter the sensitive time after an initial photoelectron pulse in order to measure and/or remove afterpulses. The dead time-corrected OR (10 μs) was used to compute PWP high voltage and electrostatic efficiency curves. The beam intensity was chosen to give peak rates on a single wire of <10 kHz to eliminate high positive ion densities which might influence the trajectories of drifting photoelectrons. A noise subtraction was made routinely by interposing a glass plate between the lamp and the TPC. Typical noise rates were less than 500 Hz.

The following sections give details of measurements made with this system to provide a better understanding of the RICH TPC performance during the 1984 run.

4.b Electrostatic collection efficiency.

In our original TPC design, (1982), the PWP sense wires were separated by 0.3 mm thick brass cathode strips. Due to mechanical construction constraints, these were replaced — with the exception of one early TPC — with 0.8 mm copper-clad fiberglass for the production TPCs.

In the following tests, the beam was positioned so that photoelectrons drifted 2 cm to the PWP structure. The beam was then scanned vertically, in 0.2 mm steps, over several cells. The corrected OR (10μs) rate showed a series of minima, coinciding with the surveyed positions of the separators. These minima deepened as the drift field was increased. A collection efficiency was calculated as the integrated beam response of the chamber across each cell divided by the integrated beam intensity derived at low drift field. The variation in collection efficiency with applied drift field is shown in Fig. 10.

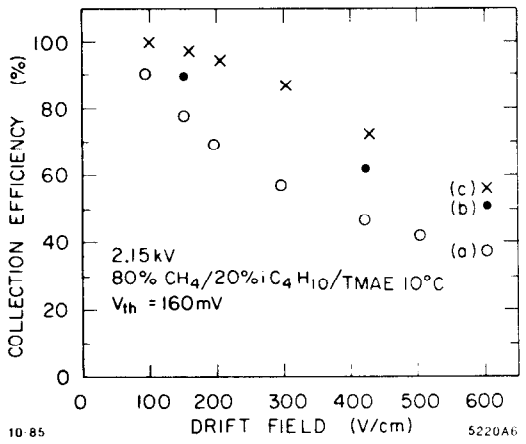

Fig. 10. TPC Electrostatic Collection Efficiency.

Three chamber configurations were tested:

a) 0.8 mm separators, with cathode wires.

b) 0.8 mm separators, without cathode wires.

c) 0.3 mm brass separators with cathode wires.

All curves show a loss of collection efficiency with increasing drift field. The difference between curves a) and b) implies losses to both separators and cathode wires. Curve c) shows that while thinner separators improve the efficiency, losses due to cathode wires are still present at high drift fields.

The collection efficiency — deduced under the 1984 running conditions of E_D = 420 V/cm, V_{PWP} = −2.15 kV — was 0.49±

0.03. Since the future background levels in which the RICH might operate are likely to be as high as those in 1984 (§5.b), an enhancement in electrostatic efficiency from a reduction in drift field is not practical (at least with the present gas mixture). Work is in progress to investigate focus structures which would improve the overall efficiency.

4.*c* Single photon detection efficiency

Pulse height spectra for single photoelectron avalanches in CH_4 have been observed to have an exponential form in the regime of low applied field and gas gain.[8] As these parameters increase the spectra develop into a peaked form which can be described by a Polya distribution.[9] The electronic threshold applied after the final stage of amplification however cuts into this distribution, leaving some fraction of it undetected.

The response of the TPC to single photoelectrons has been studied at a variety of isobutane concentrations and PWP operating voltages. The beam was aligned to ensure that the photoelectrons drifted onto a single wire. Pulse height spectra were accumulated in a multichannel analyzer from signals detected with a TSE amplifier with calibrated charge gain. Figure 11 shows the distribution of pulse charges (after the TSE amplifier) at 2.15 kV in a gas mixture of 80% CH_4 20% $iC_4H_{10}/10°C$ TMAE. The mean gas gain was estimated to be 2.5×10^5.

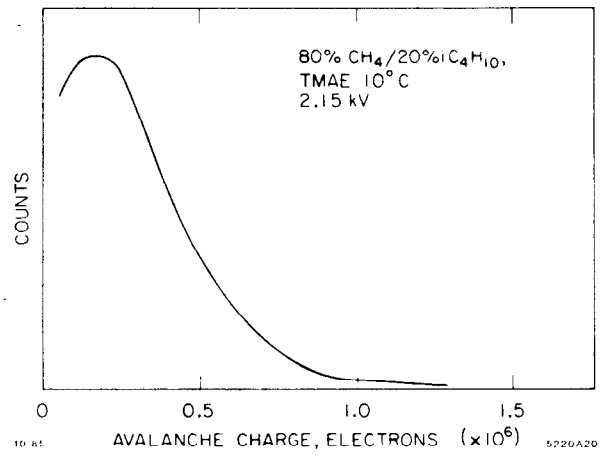

Fig. 11. TPC Single Photoelectron Pulse Height Spectrum.

The background-subtracted OR (100 ns) and OR (10 μs) count rates were measured at a variety of PWP cathode voltages for a fixed drift field of 200 V/cm. These are plotted for a TSE threshold of -160 mV in Fig. 12. The curve for OR (10 μs) at -375 mV is shown for comparison.

A divergence of OR (10 μs) and OR (100 ns)is observed at the higher voltages, indicating the on-set of afterpulsing. This effect was not observed when a similar measurement was made with no TMAE in the chamber. [In this latter case, photoelectrons were ejected from the copper end board of one of the drift volumes, using a mercury discharge lamp]. The after pulsing suppressed by the 10 μs gate has been attributed to photon feedback (§4.d).

The full beam intensity was measured to be 9.3 ± 0.4 kHz. At a cathode voltage of -2.15 kV, the single photoelectron detection efficiency was 0.88 ± 0.04 at -160 mV, and 0.72 ± 0.04 at the experimental operating threshold of -375 mV.

4.*d* Photon Feedback

The addition of TMAE to the drift gas of a TPC produces a source of afterpulsing known as photon feedback. The UV photons created in an avalanche around a sense wire propagate outwards into the drift region where they convert with high efficiency. The resulting photoelectrons then drift back to the sense plans, initiating further avalanches.

While feedback from single photoelectron avalanches adds a small background underneath the ring points, feedback from charged track ionization in the drift gas may be several hundred times greater and can cause significant background. Cathode separators are used to restrict the solid angle for escape of feedback photons and the addition of isobutane to the drift gas significantly reduces the level of feedback.

Some of the main features of photon feedback have been extracted from laboratory measurements outlined in Section 4.c. The parameter

$$F = \frac{\text{OR (100 ns)} - \text{OR (10 } \mu\text{s)}}{\text{OR (10 } \mu\text{s)}}$$

has been calculated, and represents the fraction of feedback produced by a single photoelectron avalanche which returns to the 6 adjacent wires surrounding the struck wire. The quotient removes the dependence on the single photoelectron detection efficiency, but is not corrected for electrostatic collection efficiency or electron absorbtion in the drift gas.

The dependence of the parameter F on the cathode voltage is shown in Fig. 12 and its dependence on isobutane concentration is shown in Fig. 13.

The main features observed are:

i) Feedback increases approximately exponentially with cathode voltage. The voltage at which feedback becomes self-sustaining limits the PWP operation to a point several hundred volts below the limit found in methane/isobutane mixtures without TMAE.

ii) The addition of isobutane to pure methane rapidly decreases the feedback observed but even at large concentrations of isobutane, feedback is still present.

It is of interest to understand the mechanisms of feedback photon emission in order to find the optimum conditions to limit its effect. A mechanism proposed to explain photon emission in a scintillating drift chamber containing Ar/CH_4 mixtures[10,11,12] provides a possible insight. The relevant processes which result in photon emission in the wavelength range 143.0 → 230.0 nm, between the CH_4 UV cut-off and the photoionization threshold of TMAE are:

$$e^- + CH_4 \rightarrow < CH_4 >^* \rightarrow C^* + 4H$$
$$\hookrightarrow C + h\nu$$
$$\hookrightarrow CI(156.1\ nm)$$
$$CI(165.7\ nm)$$
$$CI(193.1\ nm)$$

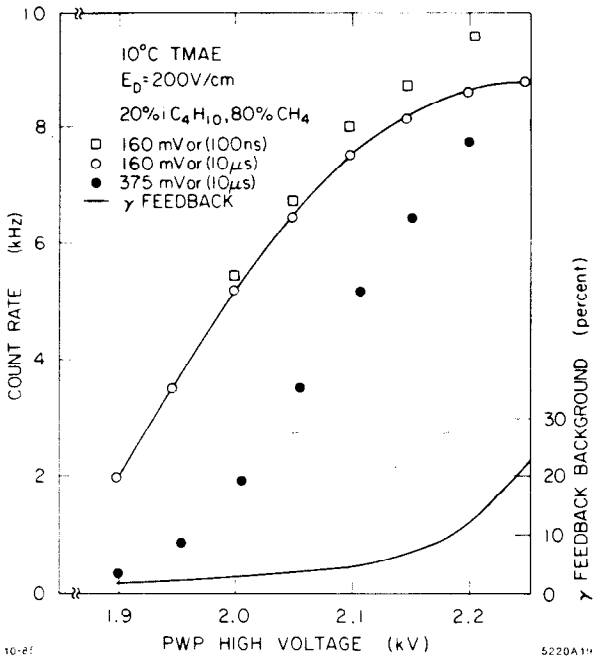

Fig. 12. Variation of Detection Efficiency and Photon Feedback with PWP Cathode High Voltage.

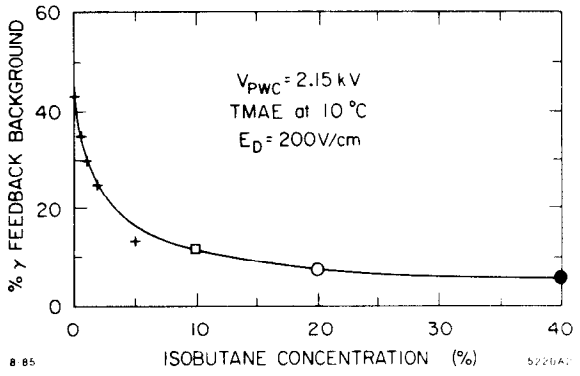

Fig. 13. Variation of Photon Feedback with Isobutane Concentration.

Figure 14 shows the position of these transitions on a plot of the transmission of 10 cm long samples of various gases. At present, however, we are unable to distinguish between a continuous or line-structured photon emission spectrum.

5. OPERATIONAL CONSIDERATIONS AND EXPERIENCE FROM THE 1984 WA69 RUN

5.*a* General Considerations

The efficient operation of any RICH is dependent on the simultaneous optimization of a large number of parameters. This optimization is difficult to achieve and maintain when transferring from the test beam or laboratory set-up to the larger scale of a complete detector.

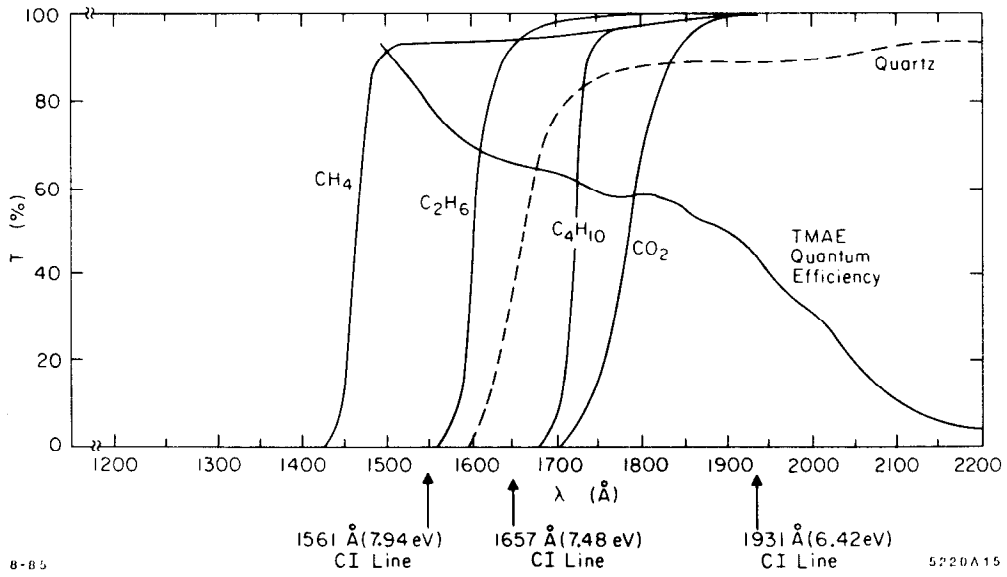

Fig. 14. Gas UV Transmission Curves, and C. I. Photon Emission Energies.

Additional constraints are placed on the detector when operating in the full experimental environment due to the large increase in beam intensity, beam-related background and electronic noise. Contradictions may arise between settings for optimal detection of single photoelectrons (i.e. a high N_o) and those required for stable, long-term operation of the TPCs: access for servicing or repairs may be restricted or even impossible.

In our experience it is essential to preselect and subsequently monitor the gases used both in the radiator and TPCs by, for example, measurement of UV transmission,[2] refractive index, oxygen and water vapour contamination and drift velocity. (§7)

5.*b* Operational experience in WA69.

The beam for the WA69 experiment delivered 2×10^5 tagged photons/sec in the energy range 70 to 180 GeV, derived from a primary 200 GeV electron beam of 3×10^6/sec. However, the total photon flux between the Čerenkov e^+e^- threshold of 21 MeV to full energy was 3.3×10^6. In addition, the flux of soft photons (from synchrotron radiation) was estimated at 5×10^6 for 21 MeV $< E\gamma <$ 100 MeV. This high instantaneous photon flux gave a significant Čerenkov background in the TPCs from e^+e^- pairs created by the conversion of photons in material upstream of the RICH radiator. Together with the ionization trails left in the TPCs by secondary particles and the effects of photon feedback, this contributed to the relatively high beam currents drawn by the TPC proportional wire planes — typically 2-4 μA at 2.15 kV and reduced the usable width of the single electron efficiency plateau. The PWP supply overcurrent trips were normally to set to 20 μA to protect the sense wires and preamplifiers, and the high voltage ramped down between SPS beam spills to reduce the incidence of overcurrent trips. The beam background was however too high to allow the TPCs to be operated with long-term stability above 2.15 kV. The TSE discriminator thresholds set at -375 mV, above the local electronic noise level, (§4.c), while the drift gas contained 20% isobutane to help stabilize the TPCs by reducing photon feedback (§4.d). This gas mixture required a drift field of about 420 V/cm for an acceptable drift velocity and sensitive time, but resulted in electrostatic losses of electrons entering the PWP (§4.b). The TMAE bubbler temperature of 15°*C* was chosen to prevent condensation within the TPCs. At this temperature, 90% of Čerenkov photons are absorbed by the TMAE.[2]

6. PRELIMINARY ANALYSIS OF THE RICH PERFORMANCE IN 1984

In order to calibrate the performance of the RICH under actual experimental running conditions, we have made a preliminary analysis of the reaction

$$\gamma p \rightarrow e^+e^-p \quad .$$

This was the dominant process in WA69, as in any photoproduction experiment, and provides a clean source of $\beta = 1$ charged particles — important in the calibration of any RICH.

The vector momentum and position of the final state leptons at the exit of the Omega Spectrometer were reconstructed by the program TRIDENT,[13] and used to predict the centres of the corresponding Čerenkov rings in the RICH TPCs.

The radial distance r_i from the predicted centre to each digitizing observed the TPCs was then used to compute a "Čerenkov Angle" θi where

$$\theta_i = r_i/f \quad ,$$

where f is the focal length: 500 cm. Assigning the electron mass, and using the track momentum to determine β, we obtain a value of refractive index n_i, or refractivity ϵ_i for each digitizing[1]

$$n_i = \frac{1}{\beta\cos\theta_i}$$

$$\epsilon_i = (n_i - 1)\times10^6$$

Figure 15 is a histogram of ϵ for e^+e^- taken under normal running conditions at a photon beam intensity of 2.5×10^5/sec, and displays the following characteristics:

i) A distinct peak at $\epsilon = 300$, determining the refractive index of the nitrogen radiator, with a width corresponding to

$$\sigma_r = 0.29 \pm 0.04 \text{ cm}$$

for the spatial resolution for photoelectrons relative to the predicted ring centre.

ii) A background level in the region of the Čerenkov peak corresponding to $\sim$ 0.04 hits / cm^2 / track in the TPCs, or a signal to background ratio of 3 within $\pm2\sigma_r$ of the expected signal. Having determined the refractive index of the radiator gas, the data were re-analyzed with a Monte-Carlo generation of the expected ring for each track. For each TPC, the Monte-Carlo points lying within the sensitive area were summed and histogrammed as a function of the drift distance from the PWP. A comparison of this distribution with that observed in the data after background subtraction (i.e. the drift distance distribution corresponding to the peak of Fig. 15) allows an estimate of the variation of $N_o$with drift distance. This is shown in Fig. 16 for a single TPC. The smooth curve is a fit to the form

$$N_o(d) = N_o(o)e^{-d/\lambda}$$

with

$$N_o(o) = 49.7 \pm 1.3$$

$$\lambda = 43.2 \pm 4.6 \text{ cm}$$

Absorbtion lengths (λ) of 45 cm were typical of all TPCs analyzed in this way, with average N_o values (over the 20 cm drift distance) of about 35 cm^{-1}.

These values of N_o give a mean number of 10.5 Čerenkov photoelectrons per $\beta = 1$ track, with an associated background of 3.5 within $\pm2\sigma_r$ of the expected ring radius.

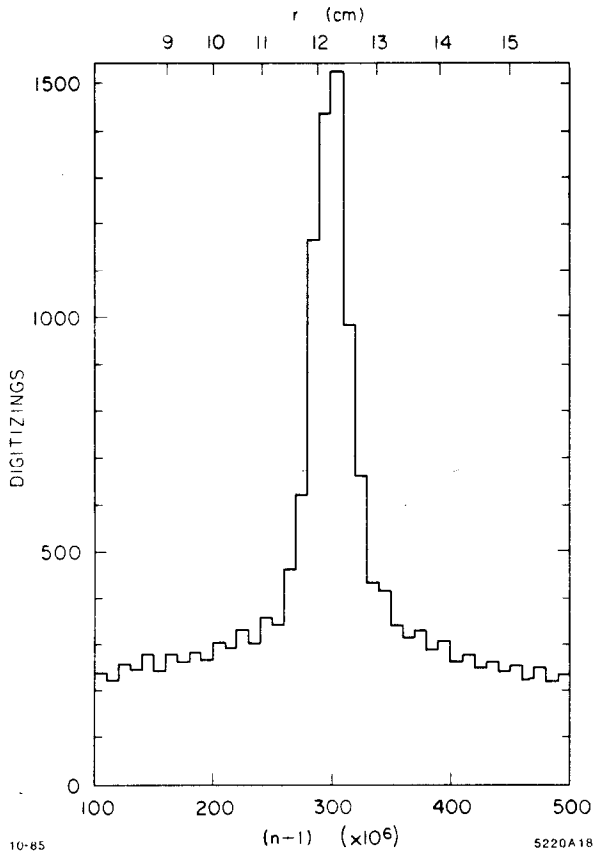

Fig. 15. Refractivity and Čerenkov Ring Radius for Identified e^+e^- Tracks.

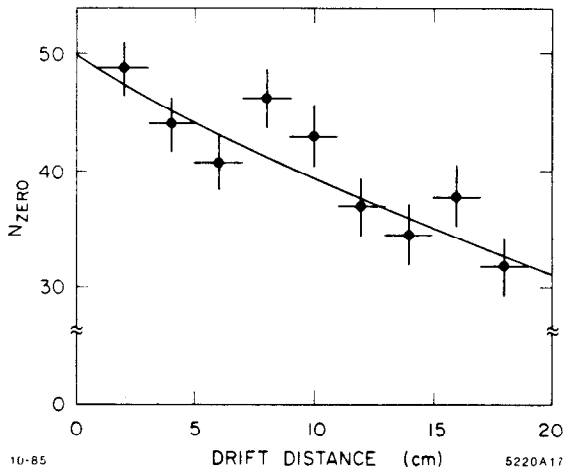

Fig. 16. Variation of N_o with Photoelectron Drift Distance.

CONCLUSIONS

We have reported on the performance of the Omega RICH in the WA69 experiment. Under normal running conditions, the RICH operated at $N_o = 35$ cm^{-1}. In a recent Monte Carlo simulation, an integration over the measured mirror UV reflectivity,[2] the transmission of the drift and radiator gases and the quartz windows,[2] the TMAE UV absorbtion length[2] and quantum efficiency,[14] predicted a value of N_o of 127 cm^{-1}.

We have estimated the overall efficiency of the TPCs under actual run conditions to be 0.28 ± 0.03 from the product of three efficiencies

i) electron drift efficiency (over average distance of 10 cm) 0.79 ± 0.02

ii) electrostatic collection efficiency 0.49 ± 0.04

iii) Single photoelectron detection efficiency 0.72 ± 0.04

Scaling the predicted N_o by the measured TPC efficiency, we obtain a value of $N_o = 36 \pm 4$ cm^{-1}, which is consistent with the measured value. Modifications have been made to upgrade the RICH performance for the second phase of WA69 in 1985:

i) a gas recirculation system has been commissioned to allow the radiator to be filled with a mixture of C_2F_6 and nitrogen. The higher refractive index will increase the Čerenkov angle, and hence N_{PE}, enabling the detector to operate at lower particle momentum thresholds.

ii) reductions in electronic noise will allow the readout system to be operated at lower effective charge thresholds

iii) the central four TPCs have been equipped with a focussing system to improve their electrostatic collection efficiency

iv) a calibration system, incorporating a pulsed UV lamp and UV transmitting optical fibres, has been installed to provide an on-line monitor of the drift velocity in each TPC.

The performance of the RICH in the 1985 run will be the subject of a future report.

ACKNOWLEDGEMENTS

We wish to thank the Rutherford Appleton Laboratory, SERC (UK) and CERN for financial and technical support for this project. We would like in particular to express our appreciation of the contribution made to this project by our late colleague Ken Freeston.

REFERENCES

1. R. J. Apsimon *et al.*, IEEE Trans. Nucl. Sci., Vol NS-32 674 (1985).
2. R. J. Apsimon *et al.*, "The Design of the Optical Components and Gas Control Systems of the CERN Omega Ring Imaging Čerenkov Detector." RAL 85-014 (Submitted to Nucl Instr & Meth).
3. G. D. Hallewell, "The Omega Ring Imaging Čerenkov Detector Readout System User's Guide," RAL-85-009.
4. P. Jarron, "Specification of the Quad Preamplifier Thick Film Hybrid Circuit for Silicon Microstrip Detectors," CERN-EF/0909H (1982).
   P. Jarron and M. Goyot, Nucl. Inst. & Meth. 226 156 (1984).
5. R. Stephenson, RAL Nuclear Physics Apparatus Group, Technical Note 66, Rutherford Appleton Laboratory Internal Report, 1975.
6. A proposal to build a Ring Imaging Čerenkov Detector for use by the Omega Photon Collaboration in WA69 PPESP/82/24 Rutherford Appleton Laboratory, April 1982.

7. D. F. Anderson, IEEE Trans. Nucl. Sci. NS-28 842 (1981).
8. H. Genz, Nucl. Inst. & Meth. 112 83 (1973).
9. G. D. Alkhazov, Nucl. Inst. & Meth. 89 155 (1970).
10. J. P. Cooch, G. K. Rochester, P. D. Smith, R. K. Sood and T. J. Sumner, IEEE Trans Nucl. Sci. Vol. NS-29 No. 5 1410 (1982).
11. G. K. Rochester, P. D. Smith, R. K. Sood and T. J. Sumner, Nucl. Inst. & Meth. 224 477 (1984).
12. H. D. Morgan and J. E. Mentall, J. Chem. Phys., 60 4734 (1974).
13. F. Carena, J-C Lassalle and S. Pensotti, Nucl. Inst. & Meth. 176 371 (1980).
14. E. Barrelet *et al.*, Nucl. Inst. & Meth. 200 219 (1982).